A.2.2

NUMERICAL MODELLING OF INVISCID

SHOCKED FLOWS OF REAL GASES

Phillip Colella
Mathematics Department
Lawrence Berkeley Laboratory
Berkeley, California 94720

Harland M. Glaz
Applied Mathematics Branch
Naval Surface Weapons Center
White Oak
Silver Spring, Maryland 20903

Eighth International Conference Numerical Methods in Fluid Dynamics, Aachen, Germany, 28 June - 2 July, 1982, ed. E. Krause, Springer-Verlag Lecture Notes in Physics, Vol. 170, 1982.

Numerical Modelling of Inviscid Shocked Flows of Real Gases*

Phillip Colella
Lawrence Berkeley Laboratory
University of California
Berkeley, California 94720

Harland M. Glaz
Naval Surface Weapons Center
White Oak Laboratory
Silver Spring, Maryland 20910

Introduction

In the past several years, there has been substantial development of various upstream-centered schemes for solving numerically the equations of inviscid compressible flow. A large subclass of these schemes rely on the existence of efficient algorithms for solving the Riemann problem. Such algorithms exist for fluids with a polytropic or isothermal equation of state, with the possible inclusion of simplified models for chemical reactions. In the following, we give a procedure for constructing solutions to the Riemann problem for fluids with a general convex equation of state. In the case where the Riemann problem is to be used to calculate fluxes for a conservative finite difference scheme, we approximate this exact Riemann solver by introducing a local parameterization of the equation of state, treating the parameters which describe the equation of state as separate dependent variables. This enables us to reduce the number of calls of the equation of state to one per zone per sweep and yields a set of algorithms for which the increase in the cost of performing a real gas calculation over that of the corresponding polytropic gas scheme, other than the single equation of state call per zone, is only a few percent. Furthermore, the real gas algorithms retain the resolution of the polytropic gas algorithms.

We consider the inviscid compressible flow equations in one space variable in conservation form

$$\frac{\partial U}{\partial t} + \frac{\partial F(U)}{\partial x} = 0$$

$$U = \begin{bmatrix} \rho \\ \rho u \\ \rho E \end{bmatrix} \qquad F(U) = \begin{bmatrix} \rho u \\ \rho u^2 + p \\ \rho u E + up \end{bmatrix}. \tag{1}$$

Here ρ is the density, u the velocity, and E the total energy per unit mass. E is the sum of the internal energy e, and the kinetic energy: $E = e + \frac{u^2}{2}$. The pressure p is derived from these quantities via an equation of state: $p = p(\tau, e)$, $\tau = \frac{1}{\rho}$.

We also need the equations (1), expressed in nonconservation form:

$$\frac{\partial V}{\partial t} + A \frac{\partial V}{\partial x} = 0$$

$$V = \begin{bmatrix} \tau \\ u \\ p \end{bmatrix} \qquad A(V) = \begin{bmatrix} u & -\tau & 0 \\ 0 & u & \tau \\ 0 & \rho c^2 & u \end{bmatrix}.$$

The adiabatic speed of sound is expressed in terms of p as $C^2 = pp_e - p_\tau$, $c = \tau C$. In the following, we will assume $C^2 > 0$ and that the equation of state is convex, i.e., $pC_e - C_\tau > 0$. The matrix $A(V)$ has left and right eigenvectors $(l_\#(V), r_\#(V))$, $l_\# \cdot r_{\#'} = \delta_{\#\#'}$, $\# = 0, +, -$, associated with the eigenvalues $\lambda_+ = u + c$, $\lambda_0 = u$,

*This research was supported by the U.S. Department of Energy, the U.S. Defense Nuclear Agency, and the Naval Surface Weapons Center Independent Research Fund.

$\lambda_- = u - c$.

The Riemann Problem

The Riemann problem is the initial value problem for (1) for which the initial data consists of two constant states separated by a single jump discontinuity.

$$U(x,0) = \begin{cases} U_L, & x < 0 \\ U_R, & x > 0 \end{cases} .$$

We look for non-entropy-decreasing solutions which depend on (x,t) only in the similarity variable $\frac{x}{t} = \xi$. Such solutions consist of four constant states separated by three waves (figure 1), each of which associated with one of the characteristic speeds. The 0-wave is a jump discontinuity in the density, across which the pressure and velocity are continuous, and which propagates at a velocity u^*. The $\pm$ waves are shock discontinuities, or centered rarefaction waves, depending on the sign of the pressure jump:

$$\begin{array}{ll} p^* > p_S & p^* < p_S \\ e(p^*, \tau_S^*) - e_S + \frac{(p_S + p^*)}{2}(\tau_S^* - \tau_S) = 0 & \frac{d\tau}{dp} = -C^2 \\ (\tau_S^* - \tau_S) + \frac{(p^* - p_S)}{W_S^2} = 0 & \frac{du}{dp} = \pm C \\ W_S(u^* - u_S) = \pm(p^* - p_S) & p_S \le p \le p^* \\ & u \pm c = \xi \end{array} \qquad (2)$$

$$(S, \pm) = (L, -), (R, +) .$$

For either a shock or a rarefaction wave, the post-wave state is uniquely determined by the pre-wave state and p^*. In particular, we can define u_S^*, the post-wave velocity, as a function of p^* and U_S. The condition that the left and right waves match up to give a solution to the Riemann problem is that $u_L^* = u_R^* = u^*$. We can also define the mean Lagrangian wave speeds

$$\begin{aligned} W_S &= \frac{p^* - p_S}{u^* - u_S} \qquad u^* \neq u_S \\ &= C_S \qquad\qquad u^* = u_S \end{aligned}$$

In the case of a shock, W_S is the quantity which appears in the shock jump relations (2). In either case, W_S is uniquely determined by U_S and p^*.

We obtain a solution to the Riemann problem by a double iteration scheme: we alternate between iterating to obtain values for W_L, W_R, given p^*, and iterating on p^* so that $u_L^* = u_R^*$. If $p^{*,l}$ is the value of p^* at the l-th iteration, then $p^{*,l+1}$ is given by

$$W_S^l = W_S(p^{*,l}, U_S)$$

$$u_S^{*,J} = u_S \pm \frac{p^{*,J} - p_S}{W_S^J}$$

$$p^{*,J+1} = p^{*,J} - (u_R^{*,J} - u_L^{*,J}) \left[\frac{p^{*,J} - p^{*,J-1}}{u_L^{*,J} - u_L^{*,J-1}} + \frac{}{u_R^{*,J} - u_R^{*,J-1}} \right].$$

This is a secant iteration corresponding to the Newton iteration in [4]. The first two guesses used to start the iteration are obtained using Godunov's iteration scheme. The calculation of W_s is performed by an iterative scheme to solve the shock jump equations if $p^* > p_s$ and by solving the ODE's using finite differences if $p^* < p_s$. The calculation of the solution as a function of $(\frac{x}{t})$ is an immediate generalization of the procedure used in the polytropic case except when $(\frac{x}{t})$ is inside a rarefaction fan. In that case, one applies inverse interpolation to the solution of the ODE's which define the solution inside the rarefaction fan as a function of the pressure.

Local Parameterization of the Equation of State

We parameterize the equation of state in terms of a function $\gamma(\rho,e)$, defined to be

$$\gamma = \frac{p(\tau,e)}{\rho e} + 1.$$

In the case of smooth flow, the behavior of γ as a function of the solution is most naturally specified along the streamline:

$$d\gamma = \left[1 - \frac{\gamma}{\Gamma} \right](\gamma - 1)\frac{1}{p}\, dp \qquad \text{along} \quad dx = u dt. \tag{3}$$

Here Γ is derived from the sound speed to be $\Gamma(\rho,e) = \frac{\rho c^2}{p}$.

In the case of discontinuities across which the Rankine-Hugoniot conditions hold, it is not possible in general to specify how γ behaves as a function of the change in the state variables without solving the equations (2). However, if the jump is not too large, then the jump relations for γ are well-approximated by an integrated form of the characteristic equations (3):

$$\gamma_S^* - \gamma_S = \left[1 - \frac{\hat{\gamma}}{\hat{\Gamma}} \right](\hat{\gamma} - 1)\, \frac{1}{\hat{p}}\, (p^* - p_S) + O(p^* - p_S)^3 \tag{4}$$

where $\hat{\gamma}$, $\hat{\Gamma}$, and $\hat{p}$ are some suitably centered values for those variables.

In order to apply this model in a specific case, we will describe how to extend the single-step Eulerian scheme given by Colella and Woodward [2] for a polytropic gas to the general equation of state case. In outline, this scheme consists of four steps:

1) the interpolation of values for the dependent variables (not necessarily the conserved quantities);
2) the construction of effective left and right states $\bar{V}_{j+\frac{1}{2},L}$, $\bar{V}_{j+\frac{1}{2},R}$ at $x_{j+\frac{1}{2}}$;
3) the solution of the Riemann problem at $x_{j+\frac{1}{2}}$ with left and right states constructed as in 2), to give $\bar{V}_{j+\frac{1}{2}}$;

4) the conservative differencing of the fluxes $F_{j+\frac{1}{2}} = F(U(\bar{V}_{j+\frac{1}{2}}))$.

$$U_j^{n+1} = U_j^n - \frac{\Delta t}{\Delta x}(F_{j+\frac{1}{2}} - F_{j-\frac{1}{2}}).$$

The states $\bar{V}_{j+\frac{1}{2}L}, \bar{V}_{j+\frac{1}{2}R}$ are constructed such that $\bar{V}_{j+\frac{1}{2}}$ is, in smooth regions, an approximation to a solution to the characteristic form of the equations at $(x_{j+\frac{1}{2}}, t^n + \frac{\Delta t}{2})$ up to terms of second order, so that the scheme is second order accurate in space and time. It is principally in steps 2) and 3) where the modifications are made to accommodate the general equation of state.

In the first step, we interpolate the variables $q = q(U_j^n)$ $q = p, \rho, u, \gamma$ using a monotonized interpolation scheme. We do not interpolate Γ but treat it as piecewise constant.

The second step is performed in two parts. First, we calculate $\tilde{V}_{j+\frac{1}{2}L}, (\tilde{V}_{j+\frac{1}{2}R})$, a first guess for the effective left (right) state, by calculating the average of U to the left (right) between the zone edge and the + (−) characteristic (figure 2). In the case where the flow is supersonic, so that there is no characteristic reaching $x_{j+\frac{1}{2}}$ from one side, we use the appropriate limiting value at $x_{j+\frac{1}{2}}$. We then make corrections to $\tilde{V}_{j+\frac{1}{2}S}$ using the characteristic projection operators (figure 3) for example, for the left state

$$\bar{V}_{j+\frac{1}{2}L} = \tilde{V}_{j+\frac{1}{2}L} - \sum_{\lambda_\#(U_j^n)>0} P^\#(\tilde{V}_{j+\frac{1}{2}L} - V^\#_{j+\frac{1}{2}L})$$

$$P^\# v = (l_\#(\tilde{V}_{j+\frac{1}{2}L})\cdot v)\, r_\#(\tilde{V}_{j+\frac{1}{2}L}) \qquad \# = +, -, 0$$

$$\bar{\gamma}_{j+\frac{1}{2}L} = \gamma^0_{j+\frac{1}{2}L} - \left[1 - \frac{\gamma_j}{\Gamma_j}\right](\gamma_j - 1)\frac{(\bar{p}_{j+\frac{1}{2}L} - p_j{}^0{}_{+\frac{1}{2}L})}{\frac{1}{2}(\bar{p}_{j+\frac{1}{2}L} + p_j{}^0{}_{+\frac{1}{2}L})} \quad \text{if } u_j^n > 0$$

$$= \tilde{\gamma}_{j+\frac{1}{2}L} \quad \text{otherwise.}$$

We calculate $\bar{V}_{j+\frac{1}{2}R}$ similarly, replacing L by R and $\lambda_\#(U_j^n)>0$ by $\lambda_\#(U_{j+1}^n)<0$.

In step 3) we solve the Riemann problem with the secant method for the general Riemann solver described above, using the model equation (4) to provide a non-iterative method for obtaining $W_S{}^2$. Given $p^*, \bar{V}_{j+\frac{1}{2}S}, \bar{\gamma}_{j+\frac{1}{2}S}$, we calculate γ_S^* to be

$$\gamma_S^* = \bar{\gamma}_{j+\frac{1}{2}S} + (1 - \frac{\hat{\gamma}}{\hat{\Gamma}})(\hat{\gamma} - 1)\frac{p^* - \bar{p}_{j+\frac{1}{2}S}}{\frac{1}{2}(p^* + \bar{p}_{j+\frac{1}{2}S})}.$$

$$\hat{\gamma} = \tfrac{1}{2}(\gamma_j^n + \gamma_{j+1}^n)$$

$$\hat{\Gamma} = \tfrac{1}{2}(\Gamma_j^n + \Gamma_{j+1}^n).$$

Given γ_S^*, it is easy to solve (2) to obtain $W_S{}^2$:

$$W_S{}^2 = \frac{(p^* - \bar{p}_{j+\frac{1}{2}S})(p^* + \frac{1}{2}(\gamma_S^* - 1)(p^* + \bar{p}_{j+\frac{1}{2}S}))}{p^*\bar{\tau}_{j+\frac{1}{2}S} - \frac{(\gamma_S^* - 1)}{(\bar{\gamma}_{j+\frac{1}{2}S} - 1)}\bar{p}_{j+\frac{1}{2}S}\bar{\tau}_{j+\frac{1}{2}S}}$$

The evaluation of the Riemann problem at $x_{j+\frac{1}{2}}$ proceeds as before, except that we use linear interpolation between the pre- and post-wave states to evaluate the solution inside a rarefaction fan.

Numerical Results

We have implemented the method described above, and tested it for a variety of equations of state. In figure 4, we show the results of a Cartesian shock tube calculation. In these results, and the figures that follow, all quantities are displayed in cgs units. The dotted line is the computed solution, and the solid line the exact solution, which was obtained using the exact Riemann solver described above. There are 180 zones in the computational domain, with the initial discontinuity located between zones 60 and 61.

The material on the left of the initial discontinuity is the product of a completely burned explosive; the material on right is air, initially at atmospheric conditions. The boundary between the two materials is tracked by solving an additional advection equation for the fraction of air in a zone. If the fraction is not 0 or 1, we take γ_j ,Γ_j in a zone to be a weighted average of those quantities for each of the two materials.

The computed solution is in good agreement with the exact solution. The slight undershoot in the internal energy to the left of the contact is a starting error, which occupies a fixed number of zones as the mesh is refined. The apparent overshoot in γ comes from evaluating the equation of state for the unphysical values of density and energy inside the shock. However, the density, energy, and pressure profiles are all monotone across the shock.

In figure 5, we show the results of the same shock tube but in spherical coordinates with the initial jump located at 3.78 cm. In this case, we see in the solution a shock and a contact discontinuity from the initial jump, as well as a second backward-facing shock which forms due to the effect of the geometry. Since this problem lacks an exact solution, we compare solutions obtained using 800 mesh points (solid line) and 400 mesh points (dotted line). The pressure is converged in the 400 zone results, but the density is not. This is not surprising, since we have only a tenth of the zones between the primary and secondary shocks to resolve the strongly varying density profile. Calculations performed previously with a constant γ EOS indicate that density profiles converge between 800 and 1600 zones.

Finally, we present in figure 6 a two-dimensional Cartesian calculation of a shock in N_2 reflecting off an oblique surface. The Mach number, shock angle, and ambient state were chosen to coincide with a shock tube experiment performed by Ben-Dor and Glass ([1], case g). We obtain the correct shock reflection pattern, that of a double Mach reflection. The wall densities are in good agreement with the experiment, except in the region just behind the shock. In the latter case, the experimental data did not resolve the detailed structure. More highly resolved experiments (Glass [3]) confirm that, at least qualitatively, the behavior seen in the present calculations is correct.

References

[1] Ben-Dor, G. and Glass, I.I., J. Fluid Mech. *92* (1979), p. 459.

[2] Colella, P. and Woodward, P.R., "The Piecewise-Parabolic Method for Gas Dynamical Simulations", in preparation.

[3] Glass, I.I., "Beyond Three Decades of Continuous Research at UTIAS on Shock Tubes and Waves", UTIAS Review, No. 45, July 1981.

[4] van Leer, B., J. Comp. Phys. *32* (1979), p. 101.

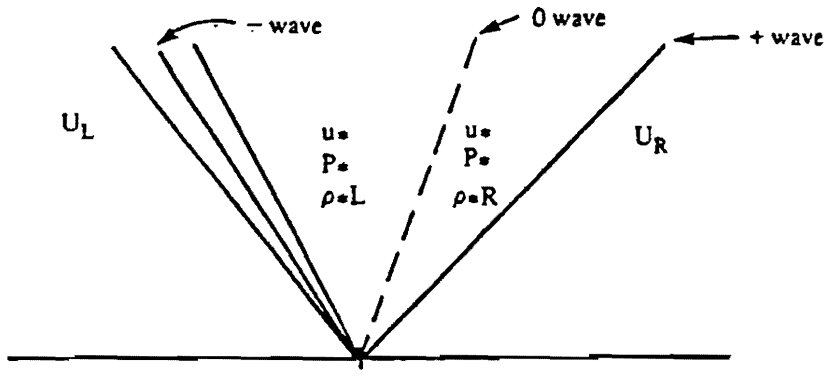

Figure 1

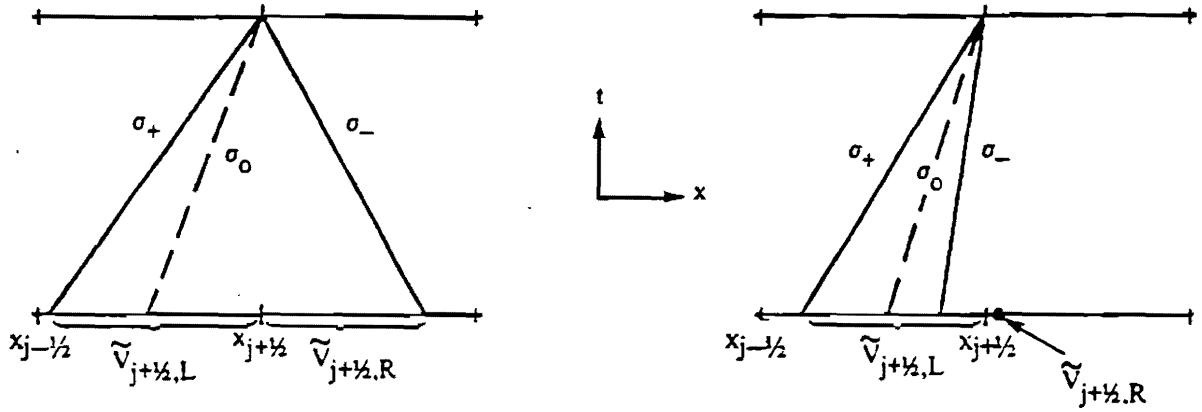

Figure 2

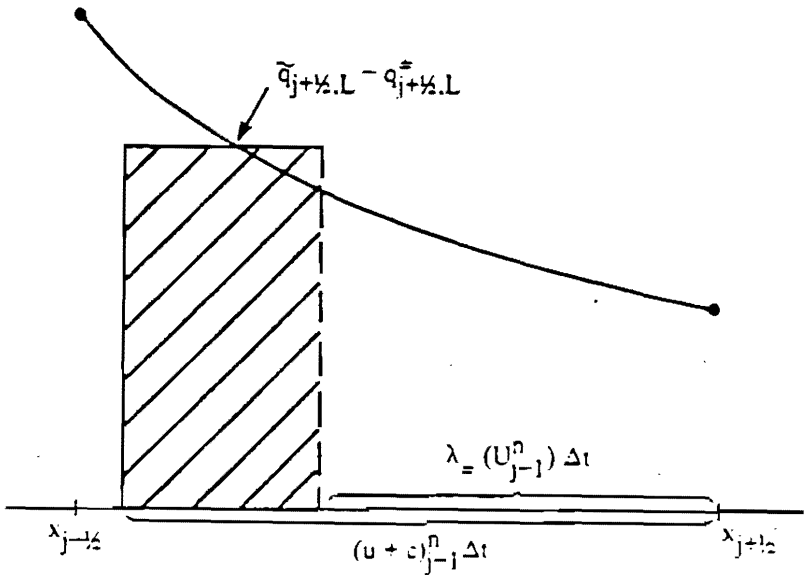

Figure 3